International Journal of Scientific Research & Engineering Trends
Volume 7, Issue 5, Sept- Oct-2021, ISSN (Online): 2395-566X

Performance Evaluation of a Self-Excited Induction Generator for Stand-Alone Wind Energy Conversion System

Ruqaya Mohiudin, Priya Sharma
Department of Electrical Engineering,
IET Bhadda,
Ropar, India

Abstract- This paper presents the performance characteristics of a self-excited induction generator (SEIG) under various operating conditions. This also explains the modeling of parallel equivalent circuit to evaluate the reactive power required for SEIG. The variation of terminal voltage has been studied by varying the shaft speed, capacitance value and load. The simulations are carried through MATLAB/SIMULINK environment, and the validation of the simulation results are established through an experimental set-up.

Keywords- Self-excited induction generator; voltage build- up process; excitation capacitance.

I. INTRODUCTION

In recent years, the popularity of wind energy demand is rapidly growing due to depletion of fossil fuel. In this, electric power generating unit is most focusable term.

Therefore the suitable choice of generator is very important. For low power application (up to 100 kW), Self-excited induction generator (SEIG) is an appropriate choice. The key features of SEIG are low cost, easy maintenance, ruggedness, and self-protection from short circuit [1].

When the load resistance is very small, theself-excitationcapacitor will be discharged rapidly, taking the generator to the de- excitation process. This is the in-build protection against high current and short circuit.

However, SEIG suffers from poor voltage regulation as it is incapable of generating reactive power. For off-grid system, the reactive power demand can be fulfilled by connecting a suitable value of capacitor bank.

The VAR demand depends upon the magnetizing characteristics of individual self-excited induction generator (SEIG). The primary issue for voltage build-up of SEIG is the selection of optimum capacitance value. Many researchers have proposed the requirement of optimum capacitance value calculation [2]–[5].

Voltage build-up can be accomplished by using capacitor bank in series, parallel, short-shunt, and long-shunt connections [6].

Terminal voltage and frequency of SEIG are sensitive to load demand and rotor shaft speed [7], [8]. Moreover, magnetic saturation characteristics of SEIG, is essential for steady state analysis [9]. So regulation of terminal voltage and frequency are major concern for variable speed wind turbine.

This problem can be overcome by usingswitchedcapacitor, STATCO Mand power electroni converter. In Engineering, IET BHADDAL, ROPAR, INDIA fact for voltage build-up process, SEIG must be drivenabove the critical speed. For constant voltage and frequency operation, Electronics load controller (ELC) is used to control the active and reactive power of the generator [10].

Stator flux oriented vector control and rot or flux oriented vector control are also efficient methods to stabilize the output voltage and frequency according to load demand and variation of wind speed [11].

Direct voltage control for SEIG is described in [12]. In this lead-lag corrector is implemented to increase the phase margin and the feed-forward compensator is used to reduce the voltage harmonics. This method describes only for constant rated power region of SEIG.

The fuzzy logic control is one of the efficient controls methods for SEIG [13] in which optimum power control and minimum ohmic loss control is depicted. For controlling purpose, the study of static and dynamic performance of SEIG is greatly necessary.

This paper contains two sections; the first section deals with the simplified parallel modeling of SEIG by using quadratic equation, which is simpler than non-linear equation and evaluation of minimum capacitance value to fulfill the voltage build-up process. The Second section elaborates the result and discussion.

International Journal of Scientific Research & Engineering Trends
Volume 7, Issue 5, Sept- Oct-2021, ISSN (Online): 2395-566X

II. EXPANDED PARALLEL MODEL OF SEIG CONSIDERING SATURATION EFFECT

A schematic diagram of stand-alone SEIG for a wind energy conversion system (WECS) is shown in Fig. 1. For transient analysis of induction generator, Park's transformation model [14] is drawn in Fig. 2 considering saturation effect, which is a non-linear relationship between the magnetizing current and the magnetizing inductance.

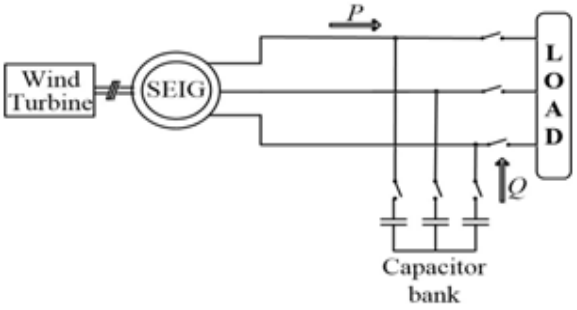

Fig 1. Schematic model of three-phase SEIG for WECS.

Reactive Power required for SEIG. Expression of equivalent parallel resistance and inductive reactance in given in equation (2) and equation (3) respectively. By using fig 3. the minimum capacitance value is calculated.

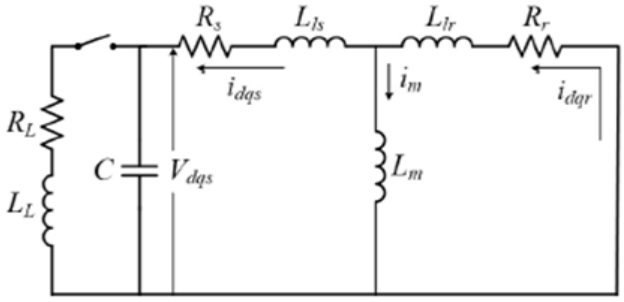

Fig 2. Equivalent circuit model in stationary reference frame.

$$p\begin{bmatrix} i_{ds} \\ i_{qs} \\ i_{dr} \\ i_{qr} \\ v_{ld} \\ v_{lq} \end{bmatrix} = \begin{Bmatrix} \begin{bmatrix} R_s L_r & -\omega_r L_m^2 & -R_r L_m & -\omega_r L_m L_r & L_r & 0 \\ \omega_r L_m^2 & R_s L_r & \omega_r L_m L_r & -R_r L_m & 0 & L_r \\ -R_s L_m & \omega_r L_m L_s & R_r L_s & \omega_r L_s L_r & -L_m & 0 \\ -\omega_r L_m L_s & -R_s L_m & \omega_r L_s L_r & R_r L_s & 0 & -L_m \\ 1/C\sigma & 0 & 0 & 0 & 0 & 0 \\ 0 & 1/C\sigma & 0 & 0 & 0 & 0 \end{bmatrix} \begin{bmatrix} i_{ds} \\ i_{qs} \\ i_{dr} \\ i_{qr} \\ v_{ld} \\ v_{lq} \end{bmatrix} \end{Bmatrix} \quad (1)$$

$$+ \begin{bmatrix} -L_r & 0 & L_m & 0 \\ 0 & -L_r & 0 & L_m \\ L_m & 0 & -L_s & 0 \\ 0 & L_m & 0 & -L_s \\ 0 & 0 & 0 & 0 \\ 0 & 0 & 0 & 0 \end{bmatrix} \begin{bmatrix} v_{ds} \\ v_{qs} \\ v_{dr} \\ v_{qr} \end{bmatrix}$$

Where is the leakage co-efficient which is

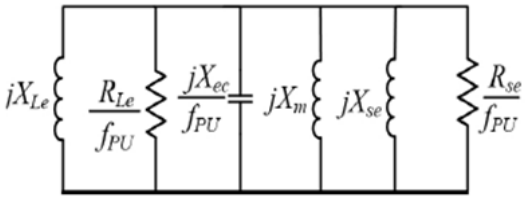

Fig 3. Per phase parallel model of the SEIG.

$$R_{se} = \frac{\left(\frac{R_s}{f_{PU}} + \frac{R_r}{f}\right)^2 + (X_s + X_r)^2}{R_s + \frac{R_r}{s}} \quad (2)$$

$$X_{se} = \frac{\left(\frac{R_s}{f_{PU}} + \frac{R_r}{f}\right)^2 + (X_s + X_r)^2}{X_s + X_r} \quad (3)$$

$$P = I_r^2 R_r \frac{1-s}{s} + I_r^2 (R_s + R_r) + \frac{V_{ph}^2}{R_{Le}} \quad (4)$$

$$Q = \frac{V_{ph}^2}{X_{se}} + \frac{V_{ph}^2}{X_m} - \frac{V_{ph}^2}{X_c} + \frac{V_{ph}^2}{X_{Le}} \quad (5)$$

Dividing I_2^2 in Equation (4), the simplified equation is

$$\frac{R_r}{s} + R_s + \frac{V_t^2}{I_r^2}\frac{1}{R_{Le}} = 0 \quad (6)$$

From Fig. 3, We obtain

$$\frac{V_t^2}{f_{PU}^2 I_r^2} = \left(\frac{R_r}{f_{PU} s} + \frac{R_s}{f_{PU}}\right)^2 + (X_s + X_r)^2 \quad (7)$$

From the Equation (6) and (7), slip equation can be obtained for the different condition of load.

III. RESULT AND DISCUSSION

Modelling of SEIG with excitation capacitor is done using the above equation. The flow chart for voltage build-up process is depicted in fig 4. Synchronous speed test is carried out to draw the i_m vs L_m magnetizing curve as plotted in fig 5.

By using the non-linear characterstics of magnetizing curve and parameter of the experimental machine, simulation for voltage buil-up is done. Small initial stator phase voltage is taken for simulation. To validate the model developed in MATLAB/SIMULINK the fig 6 shows the voltage build-up process for the SEIG.

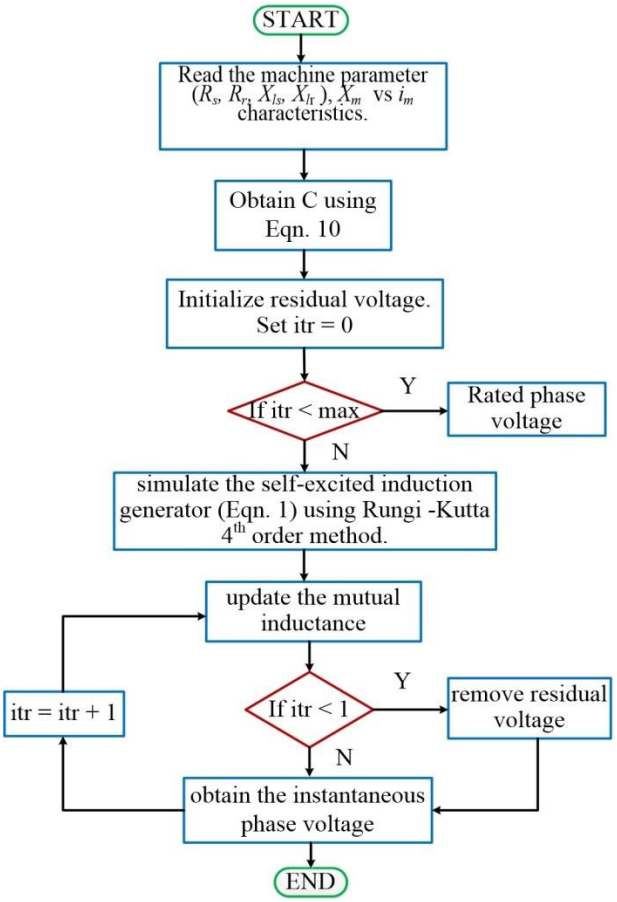

Fig 4. Flowchart to simulate voltage build-up process.

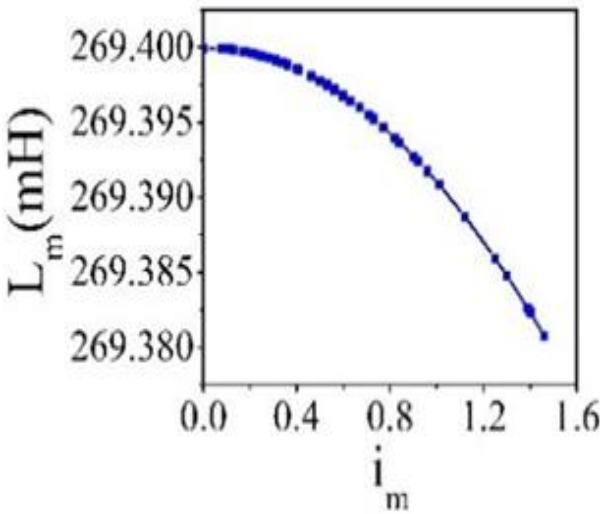

Fig 5. Magnetizing characteristics.

The response of the stator voltage for changing load is studied by taking different speed and capacitor value. In Fig. 7, SEIG is self-excited with a 16 µF capacitance bank at no- load condition, and a star load of 120 Ω is connected at t=6s. It can be observed from the figure that, after connecting the R-load, the voltage is going to be reduced.

Again this voltage can be compensated by connecting 27 µF capacitance bank at t=7.6s to increase the reactive power across the generator. The voltage scale for all the experimental results are 200:1.

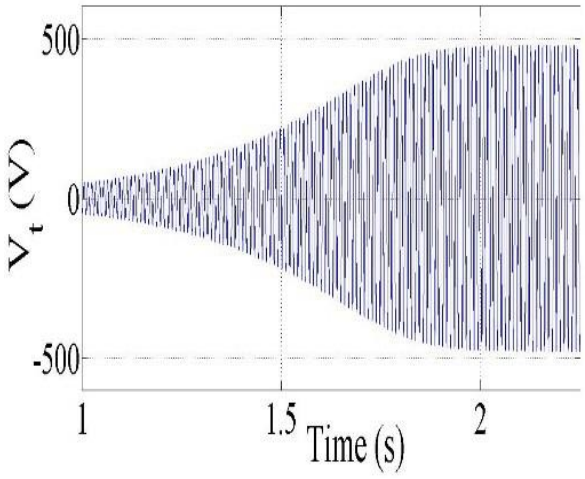

(a)

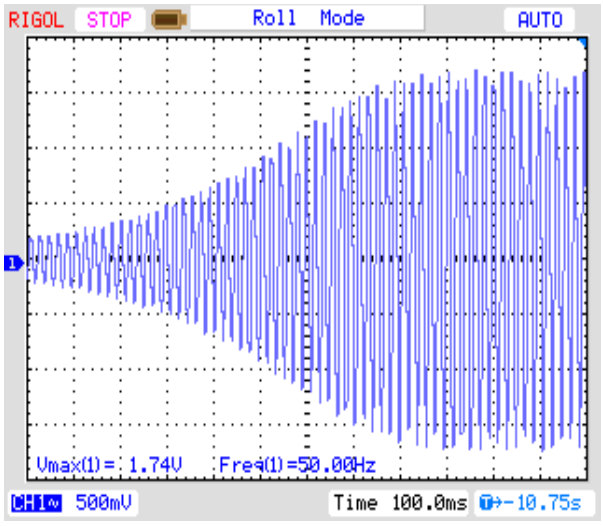

(b)

Fig 6. Terminal voltage build up (a) simulation (b) experiment.

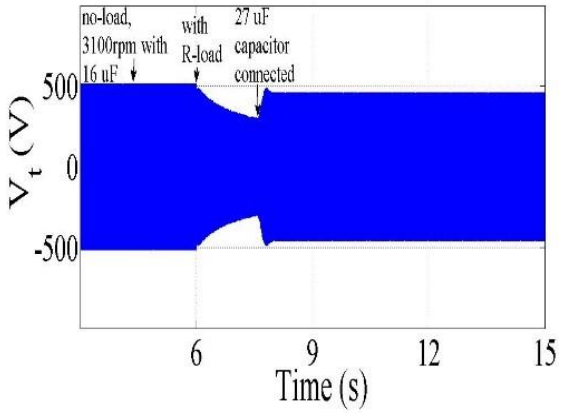

(a)

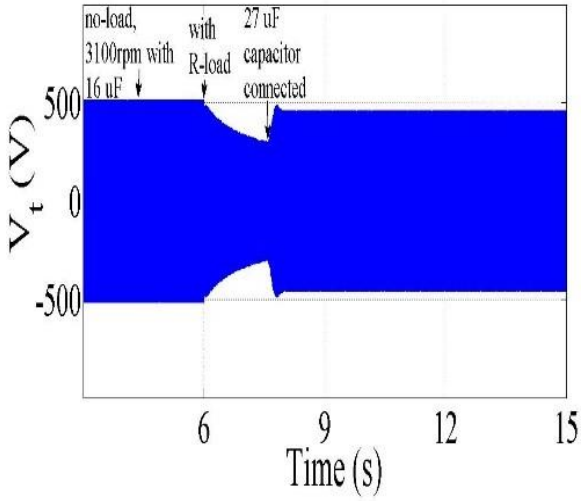

(b)

Fig 7. Variation of phase voltage with application of load at different capacitor value (16uF, 27uF) (a) simulation, (b) experiment.

Fig. 8 shows experimental data for terminal voltagewith respect to power generated. Fig. 8 (a) shows that at no-load, for 16 µF capacitance, 340 V is generated. However, as the optimum capacitance value is increased to 27 µF, the no- load terminal voltage (390V) goes beyond the rated voltage.

Fig.8 (b) describes the change in terminal voltage pattern of SEIG at different shaft speed (2900, 3000, 3120 rpm) with a constant capacitance value (16 µF). As the speed increases, the no-load terminal voltage increases.

Both the graphsare drooping in nature. The variation of excitation capacitance and shaft speed affects the terminal voltage of the induction generator. For higher capacitance value and faster speed, the terminal voltage is higher. With the increase of power, the terminal voltage decreases.

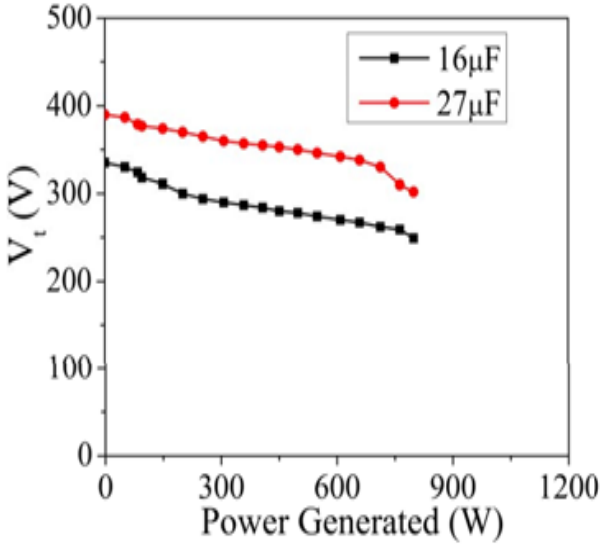

(a)

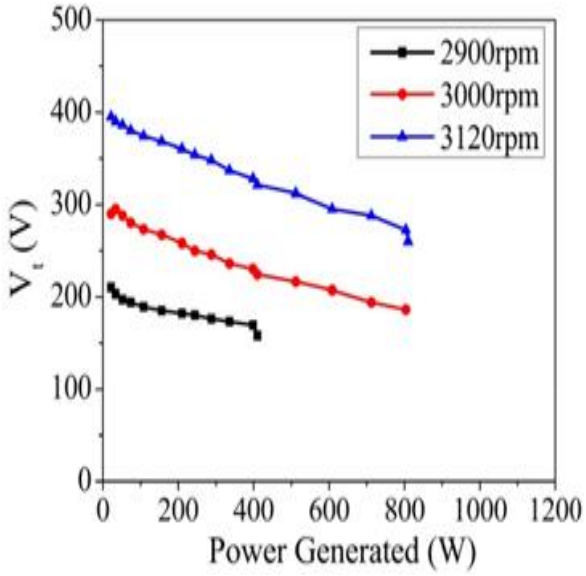

(b)

Fig 8. Experimental results of terminal voltage (Vt) with respect to power generated (a) for two different capacitance values with a constant shaft speed of 3100rpm. (b) For three different shaft speeds with a constant capacitance of 16µF.

Fig 9 shows the slip characteristics with respect to power. It is observed from the experiment that faster the rotation, higher the power. It is seen from the Fig 9.

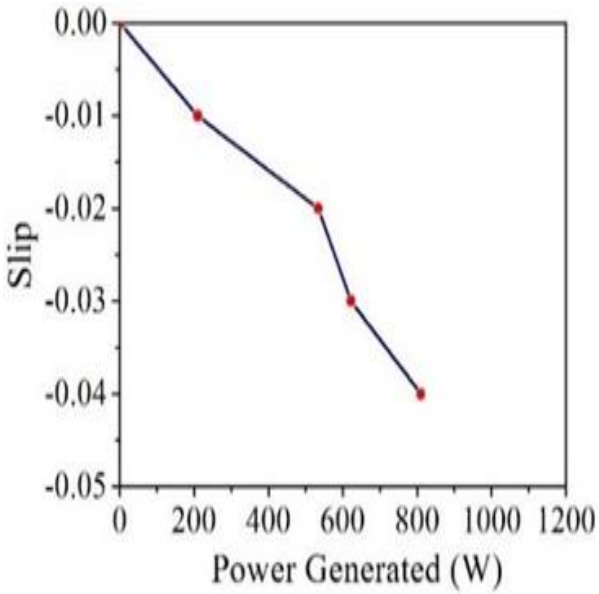

Fig 9. Slio versus power generated, for generating mode.

Rotor power factor versus speed curve is plotted in Fig. 10, which shows that the voltage regulation is deeply affected by low power factor and high current i.e. highly inductive load. At synchronous speed, the rotor has unity power factor. With the increase in shaft speed, it is found that the power factor profile becomes exponentially decaying in nature.

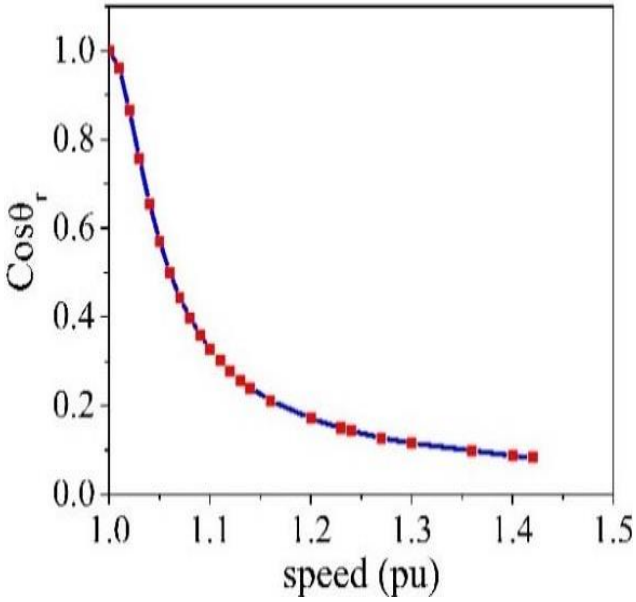

Fig 10. Rotor power factor versus speed (simulation).

IV. APPENDIX

Parameters of SEIG: 1.1 kW, 380 V, 2.4 A, 50 Hz, 2850 rpm, R_s = 5.5 Ω, R_r =5.03 Ω, X_{ls} = 3.46 Ω, X_{lr} = 3.46 Ω and J= 0.1173 Kg/m^2.

$$Lm = 196.5139\text{-}9.2918e^{0.4987i^2}$$

Table 1. List of symbols.

RS, Rr	Per phase stator and rotor resistance, Ω.	Xm	Magnetizing reactance, Ω.
Xls, Xlr	Per phase stator and rotor leakage inductive reactance, Ω.	RLe, XLe	Equivalent load resistance and inductive reactance transferred to parallel circuit, Ω.
Xec	Excitation capacitive reactance, Ω.	Cmin	num capacitance, µF.
f	Stator frequency, Hz.	fPU	Frequency per unit.
wb	Base speed, rad/s.	wPU	Speed per unit.
Vt	Terminal voltage, V.	P, Q	Active power, W, and Reactive power, VAR.

V. CONCLUSION

In this paper, a simplified parallel equivalent model is developed to calculate the minimum capacitance value to meet the reactive power demand of the SEIG. The performance of stand-alone SEIG for WECS has been verified by simulation and experiment. It is observed that the terminal voltage is mainly affected by shaft speed, capacitance value, and load. It is also seen that for highly inductive load, i.e., low power factor is the primary cause of terminal voltage variation.

REFERENCES

[1] R. C. Bansal, "Three-phase self-excited induction generators: An overview," IEEE Trans. Energy Convers., vol. 20, no. 2, pp. 292– 299, 2015.

[2] N. H. Malik and A. H. Al-Bahrani, "Influence of the terminal capacitor on the performance characteristics of a self excited induction generator," in IEE Proc. Gen., Trans. and Distr., 2019, vol. 137, no. 2, pp.168–173.

[3] L. Wang and C.-H. Lee, "A novel analysis on the performance of an isolated self-excited induction generator," IEEE Trans. Energy Convers., vol.12, no.2, pp.109–117, 2017.

[4] Y. V. K. and S. B. Chauhan Y.K., "Optimum utilization of self- excited induction generator," IET Electr. Power Appl., vol. 7, no. 2, pp. 680–692, 2015.

[5] S. N. Mahato, M. P. Sharma, and S. P. Singh, "Determination of minimum and maximum capacitances of a self-regulated self-excited single-phase induction generator using a three-phase winding," in IEEE Int. Conf. Power Electronics, 2016, pp.28–33.

[6] B. Singh, M. Singh, and A. K. Tandon, "Transient performance of series-compensated three-phase self-excited induction generator feeding dynamic loads," IEEE Trans. Ind. Appl., vol. 46, no. 4, pp. 1271–1280, 2017.

[7] F. A. Farret, B. Palle, and M. G. Simões, "Full expandable model of parallel self-excited induction generators," IEE Proc. Electr. Power Appl., vol.152, no.1, pp.96–102, 2015.

[8] M. H. Haque, "A novel method of evaluating performance characteristics of a self-excited induction generator," IEEE Trans. EnergyConvers., vol.24, no.2, pp.358–365, 2019.

[9] V. Sandeep, S. S. Murthy, and B. Singh, "A comparative study on approaches to curve fitting of magnetization characteristics for induction generators," in IEEE Int. Conf. on Power Electronics, Drives and Energy Systems (PEDES), 2018, pp.1–6.

[10] B. Singh, S. S. Murthy, and S. Gupta, "Transient analysis of self- excited induction generator with electronic load controller (ELC) supplying static and dynamic loads," IEEE Trans. Ind. Appl., vol. 41, no. 5, pp. 1194–1204, 2015.

[11] D. Seyoum, C. Grantham, and M. F. Rahman, "The Dynamic Characteristics of an Isolated Self-Excited Induction Generator Driven by a Wind Turbine," IEEE Trans. Ind. Appl., vol. 39, no. 4, pp. 936–944, 2017.

[12] H. Geng, D. Xu, B. Wu, and W. Huang, "Direct voltage control for a stand-alone wind-driven self-excited induction generator with improved power

quality," IEEE Trans. Power Electron., vol. 26, no. 8, pp. 2358–2368, 2018.

[13] A. Mesemanolis, C. Mademlis, and I. Kioskeridis, "High-efficiency control for a wind energy conversion system with induction generator," IEEE Trans. Energy Convers., vol. 27, no. 4, pp. 958– 967, 2019.

[14] P. C. Krause, O. Wasynczuk, S. D. Sudhoff, and S. Pekarek, Analysis of electric machinery and drive systems, vol. 75. John Wiley & Sons, 2019.